On linear analysis of turbulence growth rates

T.P.Kiviniemi, S.Leerink

Department of Applied Physics, Aalto University

P.O. Box 11100, 00076 AALTO, Finland

Introduction

Linear growth rate is routinely used for benchmarking activities of turbulence codes. For gyrokinetic full-f code ELMFIRE [1] this poses a challenge as it is intrinsically nonlinear full-f code where the linear growth rates of single modes can only be observed by filtering nonlinear data during or after the simulation, not by turning off terms like in other codes [3]. Another option is to look at the linear growth of macroscopic quantities like heat diffusivity or the growth of potential fluctuations without limiting the analysis to single modes. In a recent verification effort where ELMFIRE results were compared to GS2 code [4] it was also noticed that global effects have an influence on linear analysis close to the edge especially for frequencies [3]. There the frequency match improved significantly by increasing plasma current as orbit widths are narrower which decreases non-local effects. In present paper, we discuss the methods and test the code in a box-type geometry neglecting these non-local effects by turning off gradient drifts. Results are compared to recently published results on box-simulations with fully-kinetic 6D code [5].

On linear growth rate analysis

For linear codes the analysis of linear growth rates is straightforward especially if the code utilizes δf and Fourier technique to solve the equations. However, for the ELMFIRE code, which is intrinsically full-f nonlinear gyrokinetic particle-in-cell code, the linear analysis is more complicated. At least three different options for this exists: 1) Filter the mode of interest during the simulations (as in Ref. [2]), 2) Fourier analyse the nonlinear results afterwards or 3) Look at the growth rate of macroscopic quantities like particle or heat flux in the linear phase of the simulation. Filtering method was used in Ref. [2] for the code version which was using quasi-ballooning coordinates. There, only one toroidal mode was picked up which also limited the number of poloidal modes as the quasi-ballooning system optimizes the mode spectrum so that modes near the resonant criterion of resonant surface are supported (see section 5.2 of Ref. [2] for details). When filtering is not used during the run as done in Ref. [3] results are noisy. There also quasi-ballooning coordinates were not used anymore but toroidal coordinates so filtering would not have been straightforward. Third option is look at the growth of macroscopic quantities, such as heat diffusivity in Fig. 1, or the electrostatic potential fluctuation without separating single modes. For the latter one, in full-f code, the complication arises from how to define the "fluctuation" as one first needs to subtract the average of potential from the total potential to get the fluctuation. Here, results may vary depending on if this average is time average or some spatial average.

Simulation parameters

Slab-like version of the present toroidal co-centric ELMFIRE is used by neglecting the terms which depend on derivatives of magnetic field from our equations of motion in the otherwise toroidal code. Collisions are turned off. A constant magnetic field background with $B_t = 1.7T$ and $B_p = 0$ is assumed. Ion temperature in the middle of the simulation regime is $T_i(r_{mid}) = 600$ eV leading to $v_{ti} = 2.3976 \times 10^5$, $\rho_i = 1.472$ mm and $\Omega = 1.6287 \times 10^8$ (mass=1 amu) for thermal velocity, ion Larmor radius and gyrofrequency, respectively. Hyperbolic temperature profiles are assumed with $T_i(r) = T_i(r_{mid})[1 + 0.02 l_x \tanh((r_{mid} - r)/(\rho_i l_x \omega_{T_i})]$. Here, $l_x = 10\pi$ and ω_{T_i} and K_{Ti} are varied. Maxwellian distribution according this temperature profile is initialized. Adiabatic electrons with $T_e = 4T_i$ are assumed and time step is $\Delta t = 10^{-7}$ s ($\Omega\Delta t = 16.3$). Geometry parameters correspond to slab box sizes $L_x = 2$ cm, $L_y = 0.88$ m and $L_z = 11$ m respectively, and number of grid points in these directions is $30 \times 600 \times 50$ to get $\rho_i/2$ resolution in x- and ρ_i in y-direction. In the other case tested, more than doubled resolution in z-direction was tested which required coarser resolution in x- and y-direction due to memory limitation i.e. $16 \times\ 520 \times 115$ grid was used.

Results

In Fig. 1, the analysis of growth rate from heat diffusivity is shown. Between noisy start and saturation of turbulence there is phase where the heat diffusivity grows relatively linearly in logarithmic scale (similarly for potential fluctuations). This phase is here chosen by eye and results are collected to Fig. 2, where the growth rates measured from heat fluxes and potential fluctuation levels are compared. Potential fluctuation is here defined as deviation from flux surface average. Both methods are shown to give similar results. Since flux quantities are proportional to fluctuation level squared, they are divided by two in the figure. Larger discrepancies come from the different grid resolutions in the two cases. Increasing resolution in z-direction increases the growth rates even when the resolution is decreasing in the other two directions. Results are also compared to Ref. [5], where $k_{\|}\rho_i = 0.002$ and $k_{\perp}\rho_i = 0.2$ modes were resolved with $\Delta y = 0.65\rho_i$ and $\Delta z = 65.5\rho_i$ grid. In present work the grid is $\Delta x = 0.45\rho_i$, $\Delta y = \rho_i$, $\Delta z = 150\rho_i$ for the first case and $\Delta x = 0.9\rho_i$, $\Delta y = 1.15\rho_i$, $\Delta z = 65\rho_i$ for the increased reso-

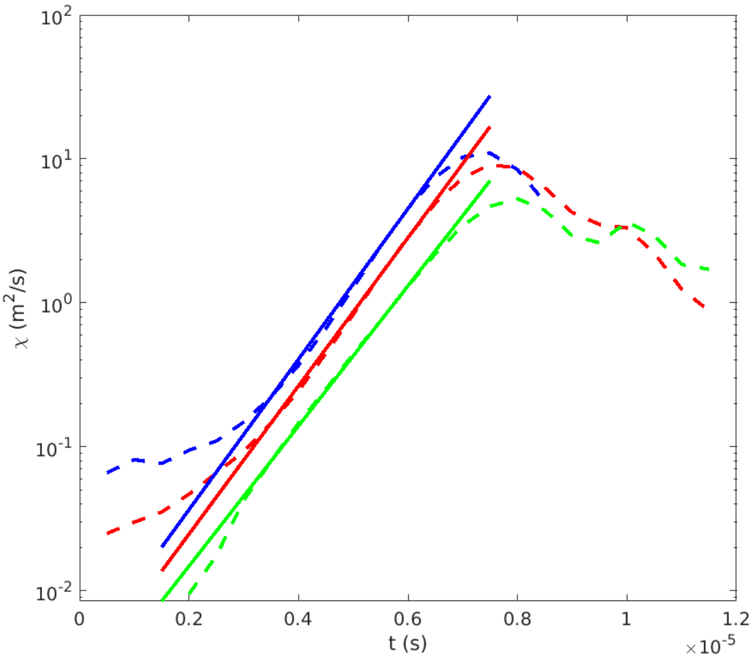

Figure 1: *Between noisy start and saturation, linear growth can be measured from linear phase of growth of heat diffusivity*

lution case. Results are matching relatively well the results of Ref. [5] being between the two simulated cases in the present work. One qualitative difference is that the simulations of present paper and relatively constant as a function of κ_T which the reference values show clear growth when κ_T increases. Reason for this difference is not yet known.

Conclusions

Linear growth rates measured from heat diffusivity gave growth rates which were, within error bars, the same as measured from potential fluctuations. Benchmark to Ref. [5] also gave relatively good agreement, but exact benchmark was not possible as same grid resolution was not possible due to memory limitations. One uncertainty rises from that slab geometry was done with toroidal code just by neglecting all the terms which depend on gradients of magnetic field. However, there may be still some geometric factors left in the LFS of equation.

Acknowledgements

The work has been supported by the Academy of Finland, grant number 316088. CSC – IT Center for Science is acknowledged for generous allocation of computational resources for this work. Katharina Kormann and Benedikt Perse are acknowledged for useful discussions.

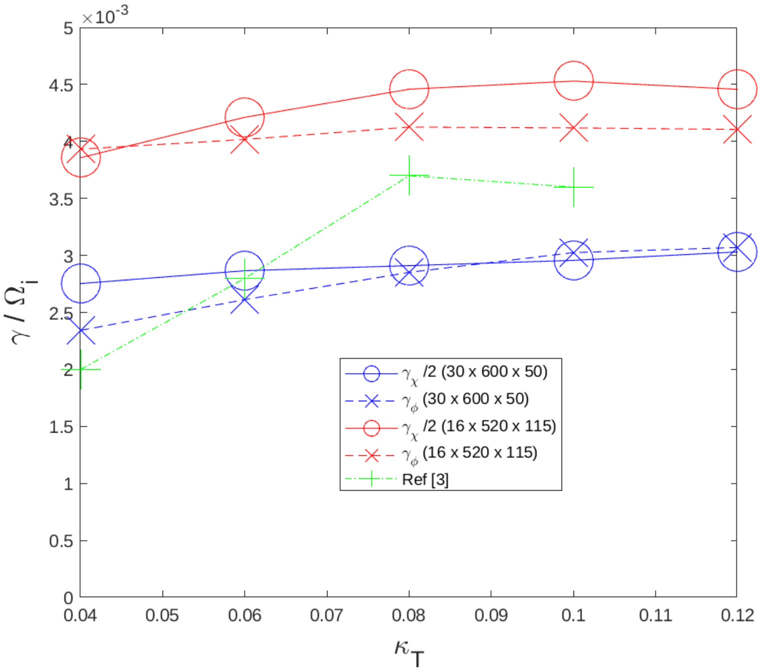

Figure 2: *Linear growth rates measured from heat diffusivity and potential fluctuation are compared to values of Ref. [5].*

References

[1] J.A. Heikkinen et al. "Full f gyrokinetic method for particle simulation of tokamak transport". In: *Journal of Computational Physics* 227, 5582 (2008), p. 5582.

[2] Salomon Janhunen. "Gyrokinetic particle simulation for thermonuclear plasma turbulence studies in magnetic confinement". In: *Doctoral thesis* (2013).

[3] T. Korpilo et al. "Gyrokinetic full-torus simulations of tokamak plasmas with limiter scrape-off-layer and wall". In: *Computer Physics Communications* 203, 128 (2016), p. 128.

[4] M. Kotschenreuther, G. Rewoldt, and W.M. Tang. "Comparison of initial value and eigenvalue codes for kinetic toroidal plasma instabilities". In: *Computer Physics Communications* 88, 128 (1995), p. 128.

[5] B.J. Sturdevant, Y. Chen, and S.E. Parker. "Low frequency fully kinetic simulation of the toroidal ion temperature gradient instability". In: *Physics of Plasmas* 24, 081207 (2017), p. 081207.